

Knowledge Distillation for Image Restoration : Simultaneous Learning from Degraded and Clean Images

Yongheng Zhang, and Danfeng Yan*

State Key Laboratory of Networking and Switching Technology, BUPT, Beijing, China

Email: zhangyongheng, yandf@bupt.edu.cn

Abstract—Model compression through knowledge distillation has seen extensive application in classification and segmentation tasks. However, its potential in image-to-image translation, particularly in image restoration, remains underexplored. To address this gap, we propose a Simultaneous Learning Knowledge Distillation (SLKD) framework tailored for model compression in image restoration tasks. SLKD employs a dual-teacher, single-student architecture with two distinct learning strategies: Degradation Removal Learning (DRL) and Image Reconstruction Learning (IRL), simultaneously. In DRL, the student encoder learns from Teacher A to focus on removing degradation factors, guided by a novel BRISQUE extractor. In IRL, the student decoder learns from Teacher B to reconstruct clean images, with the assistance of a proposed PIQE extractor. These strategies enable the student to learn from degraded and clean images simultaneously, ensuring high-quality compression of image restoration models. Experimental results across five datasets and three tasks demonstrate that SLKD achieves substantial reductions in FLOPs and parameters, exceeding 80%, while maintaining strong image restoration performance.

Index Terms—Knowledge distillation, image restoration, simultaneous learning, feature extractor

I. INTRODUCTION

Image restoration is vital in outdoor systems with limited computing resources, such as security surveillance and remote sensing satellites, making model compression essential. The concept of model compression through knowledge distillation was first introduced for image classification tasks [21] and has since been widely explored in areas like object detection [22], [23], [25]–[28]. However, unlike the feature extractor and classification projector commonly used in classification tasks, image restoration models typically employ an encoder-decoder architecture [32]. This architectural difference makes it challenging to directly apply knowledge distillation methods designed for classification tasks to image restoration.

Recent advances in knowledge distillation for compressing image transfer models [29]–[31], especially in super-resolution [33]–[35], [37], have shown promise. However, while super-resolution models primarily focus on reconstructing low-resolution images into high-resolution ones, image restoration models must first remove degradation factors (such as rain, noise, etc.) before reconstructing the image. This additional

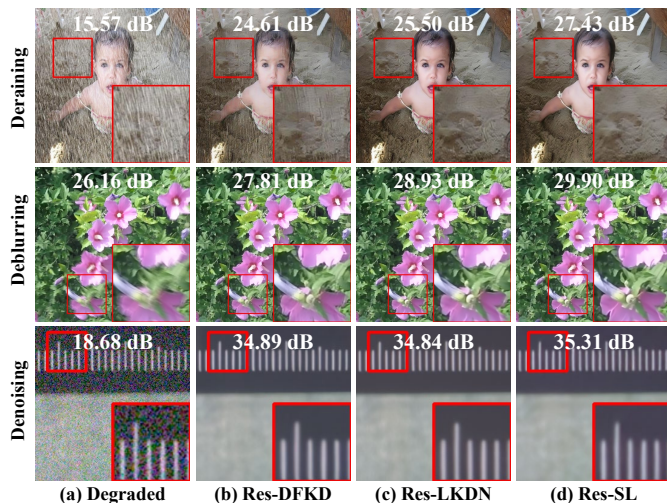


Fig. 1: Qualitative comparison with knowledge distillation methods across image deraining, deblurring and denoising.

complexity often results in suboptimal performance when using knowledge distillation methods designed for super-resolution in image restoration tasks.

Building on these insights and the specific requirements of image restoration tasks, we introduce the **Simultaneous Learning Knowledge Distillation (SLKD)** framework for compressing image restoration models. For the student encoder, we propose a **Degradation Removal Learning (DRL)** strategy, which distills knowledge from Teacher A, a network that processes degraded images. To ensure the student’s focus on degradation removal, DRL incorporates a BRISQUE-based extractor to capture scene statistical features often affected by degradation. For the student decoder, we introduce an **Image Reconstruction Learning (IRL)** strategy, which distills knowledge from Teacher B, a network that processes clean images. In IRL, a PIQE-based extractor is proposed to extract edge and texture features critical for accurate image reconstruction. These innovations enable SLKD to surpass other knowledge distillation-based model compression methods, as illustrated in Fig. 1. Experimental results across five datasets for image deraining, deblurring, and denoising, as detailed in Section III, further demonstrate SLKD’s state-of-the-art performance.

This work is supported by National Key Research and Development Program of China (No. 2021YFB3101300).

* Corresponding author (D. Yan).

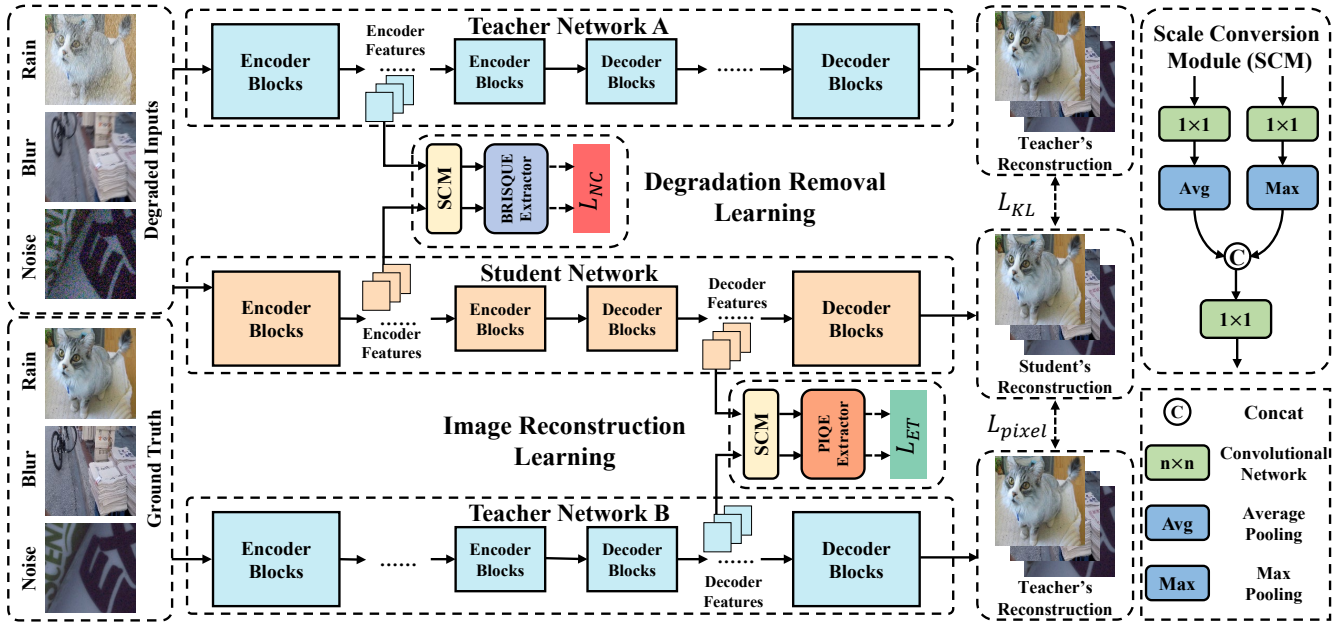


Fig. 2: The overall architecture of our proposed Simultaneous Learning Knowledge Distillation (SLKD) strategy for image restoration. SLKD includes a Degradation Removal Learning (DRL) and an Image Reconstruction Learning (IRL).

II. PROPOSED METHOD

A. Overall Architecture

As illustrated in Fig. 2, our Simultaneous Learning Knowledge Distillation (SLKD) strategy leverages two pre-trained teacher image restoration networks and a student network, which is trained by distilling knowledge from the teachers. The student network has a similar structure to the teacher networks but with fewer transformers and reduced feature dimensions in each encoder-decoder block, significantly lowering its complexity. Given a pair of degraded and clean images $I, G \in \mathcal{R}^{H \times W \times 3}$, the teacher network A and the student network both take the degraded image I as input, while the teacher network B uses the clean image G .

In the Degradation Removal Learning (DRL) strategy, the student encoder learns from the teacher A encoder, focusing on removing degradation factors and extract clean background features. This is achieved by mapping encoder features to a unified scale space using a Scale Conversion Module (SCM), followed by a BRISQUE-based extractor to capture natural scene statistics, which are used to compute the natural and color loss L_{NC} .

Similarly, in the Image Reconstruction Learning (IRL) strategy, the student decoder learns from the teacher B decoder to reconstruct a clean background image from the extracted features. The decoder features are also mapped to a unified scale space, and a PIQE-based extractor is employed to capture edge and texture features, contributing to the edge and texture loss L_{ET} .

In addition to these feature-level learning strategies, we incorporate two image-level losses: KL divergence loss and pixel-level L1 loss.

B. Degradation Removal Learning

In typical encoder-decoder architectures for image-to-image transfer tasks, the encoder gradually extracts essential features needed for the task. In the context of image restoration, these features correspond to a clean feature map, free from degradation factors. Thus, we utilize the pre-trained teacher A to restore degraded images, allowing the student encoder to learn how to progressively remove degradation by mimicking the teacher A encoder in the DRL strategy.

In DRL, a SCM first maps the k -th level encoder features from the teacher (TA_e^k) and student (S_e^k) networks into a unified scale space, resulting in TA_{eu}^k and S_{eu}^k . To ensure the student encoder focuses on removing degradation factors, we introduce a BRISQUE-based extractor to isolate natural and color features that are vulnerable to degradation. The BRISQUE-based extractor calculates Mean Subtracted Contrast Normalized (MSCN) coefficients of TA_{eu}^k and S_{eu}^k defined as:

$$\hat{I}(i, j) = \frac{I(i, j) - \mu(i, j)}{\sigma(i, j) + C}, \quad (1)$$

where $I(i, j)$ represents the pixel value at (i, j) , $\mu(i, j)$ and $\sigma(i, j)$ are the local mean and variance, respectively. The MSCN map is then used to extract natural and color features (TA_{ec}^k and S_{ec}^k) with generalized Gaussian and asymmetric generalized Gaussian distributions, as detailed in [18]. Finally, the natural and color loss L_{NC} is computed as:

$$L_{NC} = \sum_{k=1}^n \sum_{i, j} S_{ec}^k(i, j) * \log\left(\frac{S_{ec}^k(i, j)}{TA_{ec}^k(i, j)}\right), \quad (2)$$

where n is the number of encoder/decoder blocks.



Fig. 3: Qualitative comparison with light-weight methods.

C. Image Reconstruction Learning

In the encoder-decoder architecture, the decoder’s role is to gradually reconstruct the complete image from extracted features. For image restoration, this translates to producing a clear background image. To facilitate this, we use corresponding clean images as input for teacher network B , allowing the student decoder to learn how to restore edge and texture features by mimicking the teacher B decoder in the IRL.

Similarly, a SCM maps the k -th level decoder features from the teacher (TB_d^k) and student (S_d^k) networks into a unified scale space, resulting in TB_{du}^k and S_{du}^k . To ensure the student decoder focuses on reconstructing clear images, we introduce a PIQE-based extractor to capture crucial edge and texture features for image reconstruction. The PIQE-based extractor also involves MSCN coefficient calculation described in Equation (1), along with feature vector extraction. Edge and texture features (TB_{dc}^k and S_{dc}^k) are derived using distortion estimation and block variance based on the MSCN coefficients of TB_{du}^k and S_{du}^k , as detailed in [20]. The loss L_{ET} is:

$$L_{ET} = \sum_{k=1}^n \sum_{i,j} S_{dc}^k(i,j) * \log\left(\frac{S_{dc}^k(i,j)}{TB_{dc}^k(i,j)}\right), \quad (3)$$

D. Overall Loss

The image-level KL loss between student’s reconstruction S_r and teacher A ’s reconstruction TA_r is formulated as:

$$L_{KL} = \sum_{i,j} S_r(i,j) * \log\left(\frac{S_r(i,j)}{TA_r(i,j)}\right), \quad (4)$$

The pixel-level loss between student’s reconstruction S_r and teacher B ’s reconstruction TB_r is formulated as:

$$L_{pixel} = \|S_r - TB_r\|_1, \quad (5)$$

TABLE I: Hyper-parameters and complexity.

Method	layers	dim	FLOPs	Param.	Infer time
Restormer [3]	4,6,6,8	48	619.5G	26.1M	0.1103s
Res-SL	1,2,2,4	24	85.0G	3.5M	0.0356s
Uformer [2]	1,2,8,8	32	347.6G	50.9M	0.1737s
Ufor-SL	1,2,4,4	16	57.1G	7.9M	0.0540s
DRSformer [4]	4,4,6,6,8	48	972.0G	33.7M	0.3074s
DRS-SL	2,2,2,2,4	24	132.0G	4.6M	0.0599s

TABLE II: Quantitative comparison with knowledge distillation methods on five datasets.

Tasks	Deraining		Deblurring		Denoising
	Rain1400 [11]	Test1200 [12]	Gopro [13]	HIDE [14]	SIDD [15]
Restormer [3]	34.18/0.944	33.19/0.926	32.92/0.961	31.22/0.942	40.02/0.960
DFKD [33]	32.56/0.928	31.95/0.907	31.27/0.940	29.28/0.923	39.23/0.951
DCKD [37]	<u>32.67/0.930</u>	<u>32.16/0.911</u>	31.41/0.946	29.51/0.928	39.34/0.954
Res-SL	33.24/0.937	32.67/0.917	31.91/0.957	30.17/0.934	39.60/0.957
Uformer [2]	33.63/0.939	33.04/0.923	33.06/0.967	30.90/0.953	39.89/0.960
DFKD [33]	32.27/0.925	<u>32.01/0.910</u>	<u>31.60/0.949</u>	<u>29.50/0.928</u>	<u>39.27/0.952</u>
DCKD [37]	<u>32.31/0.926</u>	31.95/0.909	31.52/0.947	29.47/0.927	<u>39.28/0.952</u>
Ufor-SL	32.96/0.931	32.26/0.915	32.24/0.953	30.35/0.933	39.61/0.956
DRSformer [4]	34.33/0.947	33.31/0.927	32.76/0.958	31.17/0.940	40.03/0.960
DFKD [33]	32.59/0.929	32.17/0.911	31.21/0.938	29.33/0.924	39.22/0.951
DCKD [37]	<u>32.91/0.932</u>	<u>32.24/0.912</u>	31.44/0.945	29.41/0.926	39.27/0.951
DRS-SL	33.57/0.938	32.71/0.917	31.93/0.956	30.26/0.935	39.57/0.956

Finally, the overall loss is formulated as:

$$L_{all} = L_{pixel} + \alpha_1 L_{KL} + \alpha_2 (L_{NC} + L_{ET}). \quad (6)$$

III. EXPERIMENTS AND ANALYSIS

Datasets and Metrics. We conduct knowledge distillation experiments using five publicly available datasets: Rain1400 [11] and Test1200 [12] for deraining, Gopro [13] and HIDE [14] for deblurring, and SIDD [15] for denoising. To evaluate restoration performance, we use two full-reference metrics: Peak Signal-to-Noise Ratio (PSNR [16]) in dB and Structural Similarity Index (SSIM [17]). Model complexity is assessed by measuring FLOPs and inference time on each 512×512 image. In the tables, the best and second-best scores for the evaluated methods are highlighted and underlined.

Implementation details. Our framework is implemented in PyTorch, utilizing the Adam optimizer with parameters ($\beta_1 = 0.9$, $\beta_2 = 0.999$, weight decay $1e-4$). The models are trained for 100 epochs, starting with an initial learning rate of $1e-4$, which is gradually reduced to $1e-6$ using cosine annealing [19]. We set the batch size to 8, with a fixed patch size of 128. The trade-off weights are $\alpha_1 = 0.5$ and $\alpha_2 = 0.1$.

We select three state-of-the-art restoration methods, Restormer [3], Uformer [2], and DRSformer [4], as teacher models. The corresponding student models are named Res-SL, Ufor-SL, and DRS-SL, respectively. Table I shows the hyper-parameters (number of layers and dimensions in each layer of the encoder-decoder) of the teacher models and their corresponding student models, along with the associated re-

TABLE III: Quantitative comparison with light-weight methods on five datasets.

Methods	Rain1400 [11]	Test1200 [12]	Gopro [13]	HIDE [14]	SIDD [15]	FLOPs	Infer time
PReNet [5]	31.75/0.916	31.36/0.911	-/-	-/-	-/-	176.7G	0.0589s
RCDNet [6]	32.35/0.926	32.13/0.909	-/-	-/-	-/-	842.5G	0.1919s
DMPHN [8]	-/-	-/-	31.20/0.940	29.09/0.924	-/-	113.0G	0.0508s
MT-RNN [7]	-/-	-/-	31.15/0.945	29.15/0.918	-/-	579.0G	<u>0.0387s</u>
VDN [9]	-/-	-/-	-/-	-/-	39.28/0.956	147.9G	0.0595s
DeamNet [10]	-/-	-/-	-/-	-/-	39.47/0.957	582.9G	0.0565s
MPRNet [1]	33.64/0.938	32.91/0.916	32.66/0.959	30.96/0.939	39.71/0.958	565.0G	0.0593s
Res-SL	33.24/0.937	32.67/0.917	31.91/0.957	30.17/0.934	39.60/0.957	<u>85.0G</u>	0.0356s
Ufor-SL	32.96/0.931	32.26/0.915	<u>32.24/0.955</u>	<u>30.35/0.933</u>	<u>39.61/0.956</u>	57.1G	0.0540s
DRS-SL	<u>33.57/0.938</u>	<u>32.71/0.917</u>	31.93/0.956	<u>30.26/0.935</u>	39.57/0.956	132.0G	0.0599s

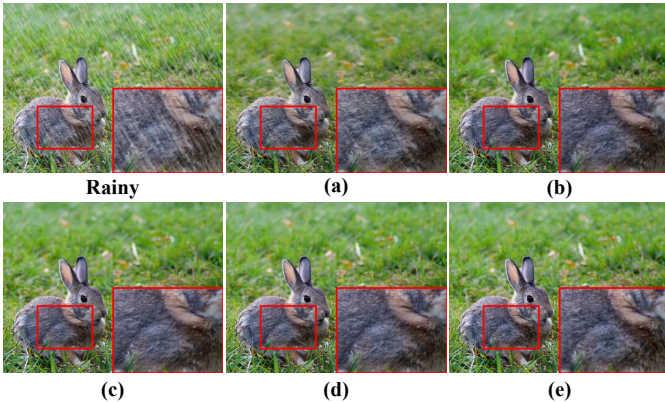


Fig. 4: Qualitative ablation study results on Rain1400 [11].

ductions in model complexity (FLOPs, inference time, number of parameters) resulting from the reduction in model size.

A. Comparisons with State-of-the-arts

We conduct a comprehensive comparison of our SLKD strategy against two SOTA image-to-image transfer knowledge distillation methods (DFKD [33], DCKD [37]) and seven lightweight SOTA restoration methods (PReNet [5], RCDNet [6], DMPHN [8], MT-RNN [7], VDN [9], DeamNet [10], MPR [1]).

Knowledge Distillation Methods. Qualitative comparisons between our strategy and the two SOTA knowledge distillation methods on three restoration tasks are presented in Fig. 1. Our strategy excels in removing multiple degradation, producing images that closely match the ground truth. Furthermore, the quantitative results, shown in Table II, reveal that our method consistently outperforms others across various teacher models and datasets, demonstrating its effectiveness.

Lightweight Methods We further evaluate our method against SOTA lightweight restoration models. Qualitative and quantitative results are displayed in Fig. 3 and Table III, respectively. In Fig. 3, it's evident that our distilled models excel at effectively mitigating multiple degradation, including rain streaks, blur, and noise. As shown in Table III, our distilled models exhibit significantly lower computational complexity compared to other models. At the same time, their performance

TABLE IV: Ablation study results on Rain1400 [11].

Sets	Source	L_{NC}	L_{ET}	PSNR/SSIM
Decoder	rainy			32.20/0.924
	clean			32.61/0.929
Loss	clean	✓		33.01/0.931
	clean		✓	32.99/0.932
Res-SL	clean	✓	✓	33.24/0.937

in terms of PSNR [16] and SSIM [17] is considerably better than that of lightweight models, approaching the performance of the more complex MPRNet [1].

B. Ablation Studies

Ablation studies are presented in Fig. 4 and Table IV. From Fig. 4 (a), (b) and corresponding first two rows in Table IV, it is evident that using clean images as input for teacher B in IRL, rather than degraded images, significantly enhances the clarity of the restored images. Additionally, as shown in Fig. 4 (b), (c), (d), (e) and corresponding rows 2-5 in Table IV, both learning strategies, along with the two losses L_{NC} and L_{ET} , independently contribute to the model's ability to remove degradation and reconstruct clean images. Together, these learning strategies significantly improve the overall quality of the restored images.

IV. CONCLUSION

In this paper, we introduce the **Simultaneous Learning Knowledge Distillation (SLKD)** framework, designed for compressing image restoration models while preserving performance. By integrating **Degradation Removal Learning (DRL)** and **Image Reconstruction Learning (IRL)**, SLKD effectively tackles the challenges of compressing image restoration models, allowing the student network to learn from both degraded and clean images. Experiments across multiple datasets and tasks, deraining, deblurring, and denoising, demonstrate that SLKD significantly reduces model complexity (over 80% fewer FLOPs and parameters) while maintaining high restoration quality. Ablation studies further validate the effectiveness of DRL and IRL in improving image clarity and overall model robustness.

REFERENCES

- [1] S. W. Zamir, A. Arora, S. Khan, M. Hayat, F. S. Khan, M.-H. Yang, and L. Shao, "Multi-stage progressive image restoration," in *Proceedings of the IEEE/CVF conference on CVPR*, 2021, pp. 14 821–14 831.
- [2] Z. Wang, X. Cun, J. Bao, W. Zhou, J. Liu, and H. Li, "Uformer: A general u-shaped transformer for image restoration," in *Proceedings of the IEEE/CVF conference on CVPR*, 2022, pp. 17 683–17 693.
- [3] S. W. Zamir, A. Arora, S. Khan, M. Hayat, F. S. Khan, and M.-H. Yang, "Restormer: Efficient transformer for high-resolution image restoration," in *Proceedings of the IEEE/CVF conference on computer vision and pattern recognition*, 2022, pp. 5728–5739.
- [4] X. Chen, H. Li, M. Li, and J. Pan, "Learning a sparse transformer network for effective image deraining," in *Proceedings of the IEEE/CVF Conference on Computer Vision and Pattern Recognition*, 2023, pp. 5896–5905.
- [5] D. Ren, W. Zuo, Q. Hu, P. Zhu, and D. Meng, "Progressive image deraining networks: A better and simpler baseline," in *Proceedings of the IEEE/CVF conference on computer vision and pattern recognition*, 2019, pp. 3937–3946.
- [6] H. Wang, Q. Xie, Q. Zhao, and D. Meng, "A model-driven deep neural network for single image rain removal," in *Proceedings of the IEEE/CVF conference on computer vision and pattern recognition*, 2020, pp. 3103–3112.
- [7] D. Park, D. U. Kang, J. Kim, and S. Y. Chun, "Multi-temporal recurrent neural networks for progressive non-uniform single image deblurring with incremental temporal training," in *European Conference on Computer Vision*. Springer, 2020, pp. 327–343.
- [8] H. Zhang, Y. Dai, H. Li, and P. Koniusz, "Deep stacked hierarchical multi-patch network for image deblurring," in *Proceedings of the IEEE/CVF conference on computer vision and pattern recognition*, 2019, pp. 5978–5986.
- [9] Z. Yue, H. Yong, Q. Zhao, D. Meng, and L. Zhang, "Variational denoising network: Toward blind noise modeling and removal," *Advances in neural information processing systems*, vol. 32, 2019.
- [10] C. Ren, X. He, C. Wang, and Z. Zhao, "Adaptive consistency prior based deep network for image denoising," in *Proceedings of the IEEE/CVF conference on computer vision and pattern recognition*, 2021, pp. 8596–8606.
- [11] X. Fu, J. Huang, D. Zeng, Y. Huang, X. Ding, and J. Paisley, "Removing rain from single images via a deep detail network," in *CVPR*. IEEE, 2017, pp. 3855–3863.
- [12] H. Zhang and V. M. Patel, "Density-aware single image de-raining using a multi-stream dense network," in *Proceedings of the IEEE conference on computer vision and pattern recognition*, 2018, pp. 695–704.
- [13] S. Nah, T. Hyun Kim, and K. Mu Lee, "Deep multi-scale convolutional neural network for dynamic scene deblurring," in *Proceedings of the IEEE conference on computer vision and pattern recognition*, 2017, pp. 3883–3891.
- [14] Z. Shen, W. Wang, X. Lu, J. Shen, H. Ling, T. Xu, and L. Shao, "Human-aware motion deblurring," in *Proceedings of the IEEE/CVF international conference on computer vision*, 2019, pp. 5572–5581.
- [15] A. Abdelhamed, S. Lin, and M. S. Brown, "A high-quality denoising dataset for smartphone cameras," in *Proceedings of the IEEE conference on computer vision and pattern recognition*, 2018, pp. 1692–1700.
- [16] Q. Huynh-Thu and M. Ghanbari, "Scope of validity of psnr in image/video quality assessment," *Electronics letters*, vol. 44, no. 13, pp. 800–801, 2008.
- [17] Z. Wang, A. C. Bovik, H. R. Sheikh, and E. P. Simoncelli, "Image quality assessment: from error visibility to structural similarity," *IEEE transactions on image processing*, vol. 13, no. 4, pp. 600–612, 2004.
- [18] A. Mittal, A. K. Moorthy, and A. C. Bovik, "No-reference image quality assessment in the spatial domain," *IEEE Transactions on image processing*, vol. 21, no. 12, pp. 4695–4708, 2012.
- [19] I. Loshchilov and F. Hutter, "Sgdr: Stochastic gradient descent with warm restarts," *arXiv preprint arXiv:1608.03983*, 2016.
- [20] N. Venkatanath, D. Praneeth, M. C. Bh, S. S. Channappayya, and S. S. Medasani, "Blind image quality evaluation using perception based features," in *NCC*. IEEE, 2015, pp. 1–6.
- [21] G. Hinton, O. Vinyals, and J. Dean, "Distilling the knowledge in a neural network," *arXiv preprint arXiv:1503.02531*, 2015.
- [22] A. Romero, N. Ballas, S. E. Kahou, A. Chassang, C. Gatta, and Y. Bengio, "Fitnets: Hints for thin deep nets," *arXiv preprint arXiv:1412.6550*, 2014.
- [23] S. Zagoruyko and N. Komodakis, "Paying more attention to attention: Improving the performance of convolutional neural networks via attention transfer," *arXiv preprint arXiv:1612.03928*, 2016.
- [24] R. Li, R. T. Tan, and L.-F. Cheong, "All in one bad weather removal using architectural search," in *Proceedings of the IEEE/CVF conference on CVPR*, 2020, pp. 3175–3185.
- [25] C. Yang, L. Xie, C. Su, and A. L. Yuille, "Snapshot distillation: Teacher-student optimization in one generation," in *Proceedings of the IEEE/CVF Conference on Computer Vision and Pattern Recognition*, 2019, pp. 2859–2868.
- [26] B. Zhao, Q. Cui, R. Song, Y. Qiu, and J. Liang, "Decoupled knowledge distillation," in *Proceedings of the IEEE/CVF Conference on computer vision and pattern recognition*, 2022, pp. 11 953–11 962.
- [27] J. Wang, Y. Chen, Z. Zheng, X. Li, M.-M. Cheng, and Q. Hou, "Crosskd: Cross-head knowledge distillation for object detection," in *Proceedings of the IEEE/CVF Conference on Computer Vision and Pattern Recognition*, 2024, pp. 16 520–16 530.
- [28] J. Kim, S. Park, and N. Kwak, "Paraphrasing complex network: Network compression via factor transfer," *Advances in neural information processing systems*, vol. 31, 2018.
- [29] L. Zhang, X. Chen, X. Tu, P. Wan, N. Xu, and K. Ma, "Wavelet distillation: Towards efficient image-to-image translation," in *Proceedings of the IEEE/CVF conference on computer vision and pattern recognition*, 2022, pp. 12 464–12 474.
- [30] Z. Li, R. Jiang, and P. Aarabi, "Semantic relation preserving knowledge distillation for image-to-image translation," in *Computer Vision—ECCV 2020: 16th European Conference, Glasgow, UK, August 23–28, 2020, Proceedings, Part XXVI 16*. Springer, 2020, pp. 648–663.
- [31] Q. Jin, J. Ren, O. J. Woodford, J. Wang, G. Yuan, Y. Wang, and S. Tulyakov, "Teachers do more than teach: Compressing image-to-image models," in *Proceedings of the IEEE/CVF Conference on Computer Vision and Pattern Recognition*, 2021, pp. 13 600–13 611.
- [32] O. Ronneberger, P. Fischer, and T. Brox, "U-net: Convolutional networks for biomedical image segmentation," in *Medical image computing and computer-assisted intervention—MICCAI 2015: 18th international conference, Munich, Germany, October 5–9, 2015, proceedings, part III 18*. Springer, 2015, pp. 234–241.
- [33] Y. Zhang, H. Chen, X. Chen, Y. Deng, C. Xu, and Y. Wang, "Data-free knowledge distillation for image super-resolution," in *Proceedings of the IEEE/CVF Conference on Computer Vision and Pattern Recognition*, 2021, pp. 7852–7861.
- [34] Q. Gao, Y. Zhao, G. Li, and T. Tong, "Image super-resolution using knowledge distillation," in *Asian Conference on Computer Vision*. Springer, 2018, pp. 527–541.
- [35] Z. Hui, X. Wang, and X. Gao, "Fast and accurate single image super-resolution via information distillation network," in *Proceedings of the IEEE conference on computer vision and pattern recognition*, 2018, pp. 723–731.
- [36] C. Xie, X. Zhang, L. Li, H. Meng, T. Zhang, T. Li, and X. Zhao, "Large kernel distillation network for efficient single image super-resolution," in *Proceedings of the IEEE/CVF Conference on Computer Vision and Pattern Recognition*, 2023, pp. 1283–1292.
- [37] H. Fang, Y. Long, X. Hu, Y. Ou, Y. Huang, and H. Hu, "Dual cross knowledge distillation for image super-resolution," *Journal of Visual Communication and Image Representation*, vol. 95, p. 103858, 2023.